INTERNATIONAL JOURNAL FOR NUMERICAL METHODS IN FLUIDS
Int. J. Numer. Meth. Fluids 2002; **40**:121–136 (DOI: 10.1002/fld.336)

Adaptive grid generation by minimizing residuals

Philip Roe*,† and Hiroaki Nishikawa

W.M. Keck Foundation Laboratory for Computational Fluid Dynamics, Department of Aerospace Engineering, University of Michigan, FXB Building, 1320 Beal Avenue, Ann Arbor, MI 48109-2140, U.S.A.

SUMMARY

We describe recent developments in the method of fluctuation splitting, in particular the minimization of residuals with respect to both the nodal values of the solution and also the nodal co-ordinates. For elliptic problems, including external (lifting) flows, obtaining good results requires that the residuals be evaluated to third order. Solutions to typical airfoil problems can then be obtained with very economical grids. For hyperbolic problems, only a second-order evaluation of the residual is needed. Shocks can be incorporated with arbitrarily high resolution by allowing elements to shrink to zero area, but to exclude the possibility of rarefaction shocks an adaptive quadrature must be employed. Copyright © 2002 John Wiley & Sons, Ltd.

1. INTRODUCTION

Computational strategies for partial differential equations (PDEs) require some kind of grid on which to represent the discrete solution. Increasingly, to represent complex behaviour in three dimensions without using excessive resources, these grids must be in some sense adapted to the problem at hand. There are many ways in which this can be done, and probably no universal recipe is best for all cases. This paper deals with unstructured simplex grids (triangular or tetrahedral elements) with the solution stored at the vertices. What does a 'good' grid of this type look like?

A naive view of the ideal grid would be the one in Figure 1, composed of uniform equilateral triangles. Of course, such a grid offers no degrees of freedom with which to adapt, but one starts off with an intuitive assumption that a good grid 'looks as much like Figure 1 as possible'. In particular, no element should have any angle that is either very small or very obtuse, and most vertices should be the meeting point of six elements. This, however, is mere aesthetics, and takes no account of

1. The geometry of the boundary.
2. The nature of the solution (smooth or non-smooth, isotropic or oriented).
3. The PDEs being solved (elliptic or hyperbolic, linear or non-linear).

*Correspondence to: P. Roe, Department of Aerospace Engineering, University of Michigan, FXB Building, 1320 Beal Avenue, Ann Arbor, Michigan 48109-2140, U.S.A.
†E-mail: philroe@engin.umich.edu

Received May 2001
Revised September 2001

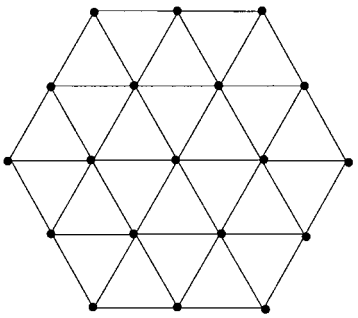

Figure 1. Naive considerations might lead us to suppose that an unstructured grid would look as much like this as possible.

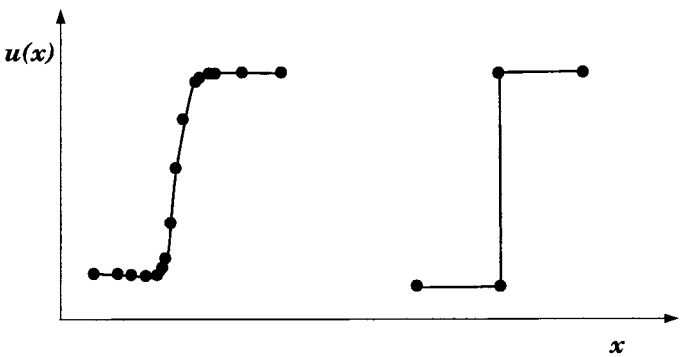

Figure 2. The use of curvature-related refinement leads to redundant representation of simple discontinuities (left). The ideal captured shock would be as shown on the right.

We will not concern ourselves much with item 1, since the boundary is known to begin with, and it is fairly clear what constraints it imposes. Considering the nature of the solution usually leads to a clustering of the grid points based either on gradients or second derivatives of the solution, estimated of course from the discrete solution itself. Since a vertex-based finite-element representation is exact for any linear function, however steep, it is usually curvature-related criteria that are applied to the sort of storage we consider. An ambitious example is presented in Reference [6], based on earlier work by Castro-Diaz *et al.* [3]. A drawback of such methods is that they interpret shocks or other discontinuities as regions of intense curvature, and therefore pack them densely with grid points. This would be fine if we needed to resolve the internal shock structure, but much more often we would be content with the shock represented as a discontinuity. This could be done much more economically (Figure 2). Similar points are made in Reference [11] which also contains a useful literature survey.

A way to clarify the requirements is to consider the nature of the governing equations. If these are hyperbolic, it may be that discontinuities are to be expected, and not all intense

curvature should call for dense grids. In fact, the orientation of the grid edges relative to the characteristics may be even more important than the grid density. Could there be an approach that takes all of this into account?

In 1995, the first author was inclined to think that it might be rather easy [9]. Residual Distribution schemes for solving steady-state problems begin each iteration by computing a residual for each element and then distributing it to the vertices of that element. Changes accumulate at each node due to changes received from all elements meeting at that node. In the Fluctuation–Splitting method, the residual, or fluctuation, of each element is distributed to its nodes in such a way as to reflect the local physics. Suppose that the residual is used to drive changes not only in the nodal value of the solution, but also in the co-ordinates of the nodes.

For example, minimization of the residuals in some suitable norm by a steepest descent method is of precisely this form if the minimization is with respect to both the solution $\{\mathbf{u}_j\}$ and also the nodal co-ordinates $\{\mathbf{x}_j\}$. This strategy led to spectacular success in its first application. For a linear (not necessarily constant-coefficient) scalar problem it turns out that the residuals vanish if one side of an element is characteristic, and if the solution is constant along that side. Any procedure that minimizes residuals automatically finds such a solution; it converts the grid into a characteristic grid and then finds an exact solution on it. Although the simple steepest-descent method is unbearably slow to converge, a simple modification makes the method very fast [1]. The same ability to find exact solutions holds for 2×2 linear hyperbolic systems.

Further, for arbitrary sets of non-linear conservation laws, if the quadrature is performed in a certain way, then the residual vanishes if the solution is identical at two vertices, satisfies a Rankine–Hugoniot condition at the third, and if a side of the element is aligned with the direction of the corresponding jump. This gives the method a potential ability to represent captured shocks and other allowable discontinuities as arbitrarily narrow jumps, two- (or three-) dimensional versions of the discontinuity in Figure 2. The practical implementation of this idea met some obstacles. Initial efforts by the present authors fell foul of instabilities. Additionally, there seemed no reason why the method should not generate entropy-violating shocks. Baines *et al.* [1, 2] nevertheless succeeded in obtaining excellent solutions of shocked flows by flagging those cell interfaces that would be required to represent the shocks, and adopting special relaxation procedures for them.

A further difficulty arose with the solution of elliptic problems expressed as first-order systems, for example the Cauchy–Riemann equations. The analysis in Reference [9] was promising. Minimizing the residuals of the Cauchy–Riemann system in a certain norm gave, in the steady state, a discretization identical to that obtained by applying the standard Galerkin discretization to the pair of equivalent Laplace equations. The only issue, apparently, was the correct boundary discretization to couple the two Laplace solutions. This proved remarkably elusive, even for a fixed grid, especially in the interesting case that the flow involved non-zero circulation. Moreover, the use of mesh refinement did little, if anything, to improve the solution. We concluded that (a) residual minimization is not always an effective technique for elliptic problems and (b) unlike the hyperbolic case, the size of the residual is not a good indicator of the local error. However, an upgrade of the method to third order solved both problems.

This paper brings the story up to date. The generally optimistic conclusion of Reference [9] was that everything was possible by minimizing the right functional in the right norm.

Without going back on that, it has to be confessed that finding those functionals and norms has proved to be a much subtler business than anticipated. Nevertheless, all of the fundamental building blocks now seem to be in place. We will present calculations for some simple but varied situations that are remarkably well-resolved on rather coarse grids. However, we have not yet given much attention to deriving these grids by economical procedures, and it also remains to synthesize them into a practical code.

2. FLUCTUATIONS

Consider the equation

$$a\partial_x u + b\partial_y u = 0 \tag{1}$$

where a, b are for the moment constants, either scalar- or matrix-valued. When they are specifically matrices, bold type will be used. The application to non-linear problems is by elementwise linearization [5]. Define the fluctuation ϕ^T associated with a triangular element T to be

$$\begin{aligned}
\phi^T &= \iint (a\partial_x u + b\partial_y u)\,\mathrm{d}x\,\mathrm{d}y, \\
&= \text{by Gauss' Theorem } \oint (au\,\mathrm{d}y - bu\,\mathrm{d}x) \\
&= a\left[\frac{u_1+u_2}{2}(y_2-y_1) + \frac{u_2+u_3}{2}(y_3-y_2) + \frac{u_3+u_1}{2}(y_1-y_3)\right] \\
&\quad - b\left[\frac{u_1+u_2}{2}(x_2-x_1) + \frac{u_2+u_3}{2}(x_3-x_2) + \frac{u_3+u_1}{2}(x_1-x_3)\right]
\end{aligned} \tag{2}$$

This expression can be put into a great number of useful alternative forms, some of which are asymmetric, for example

$$\phi^T = \tfrac{1}{2}[b(x_2-x_3) - a(y_2-y_3)](u_2-u_1) + \tfrac{1}{2}[b(x_2-x_1) - a(y_2-y_1)](u_3-u_2) \tag{3}$$

If a, b, u are scalar, each of the bracketed quantities in (3) vanishes if the corresponding edge is characteristic ($\mathrm{d}y/\mathrm{d}x = b/a$), so for any element having one characteristic side, one term in this expression will be zero. If, additionally, the characteristic equation $\mathrm{d}u = 0$ is satisfied along this edge, then the other term is also zero. Cyclic permutation of the formula shows (of course) that any one of the three sides might be characteristic. For three-dimensional advection problems, the corresponding result is that the residual vanishes if any edge of a tetrahedral element is characteristic.

The corresponding result for a 2×2 hyperbolic system follows from recalling that (1) is hyperbolic if it has simple wave solutions $u = F(y - \lambda x)$, which is possible if the generalized eigenvalue problem $(\lambda\mathbf{a} - \mathbf{b})\mathbf{r} = 0$ has two independent solutions $(\lambda_1\mathbf{a} - \mathbf{b})\mathbf{r}_1 = 0$, $(\lambda_2\mathbf{a} - \mathbf{b})\mathbf{r}_2 = 0$. So the residual vanishes if $(y_2 - y_3)/(x_2 - x_3) = \lambda_1, \mathbf{u}_2 - \mathbf{u}_3 \propto \mathbf{r}_1$ and $(y_2 - y_1)/(x_2 - x_1) = \lambda_2$, $\mathbf{u}_2 - \mathbf{u}_1 \propto \mathbf{r}_2$. This implies that $\mathbf{u}_2, \mathbf{u}_3$ satisfy the characteristic equation $\mathbf{l}_1(\mathbf{u}_2 - \mathbf{u}_3)$ where $\mathbf{l}_1$ solves

$\mathbf{l}_1(\lambda_1\mathbf{a}-\mathbf{b})=0$. Similarly, $\mathbf{u}_2,\mathbf{u}_1$ satisfy the characteristic equation $\mathbf{l}_2(\mathbf{u}_2-\mathbf{u}_1)$ where $\mathbf{l}_2$ solves $\mathbf{l}_2(\lambda_2\mathbf{a}-\mathbf{b})=0$. The corresponding result in three dimensions, for a 3×3 system, is that if three faces of a tetrahedral element are tangent to the Mach cone, the residual vanishes if the characteristic compatibility condition is satisfied within all such faces.

To know whether such grids can be achieved, it is useful to take Euler's equation for the numbers C,E,V of cells, edges and vertices of any two-dimensional graph,

$$C-E+V=1$$

together with the formula, valid for any triangular graph,

$$3C=2E_{\mathrm{i}}+E_{\mathrm{b}}$$

where $E_{\mathrm{i}},E_{\mathrm{b}}$ are, respectively, the number of edges in the interior and on the boundary. In the scalar case, with a fixed grid, the number of equations to be satisfied is C. The number of unknowns is $V-V_{\mathrm{b,in}}$ where $V_{\mathrm{b,in}}$ is the number of vertices on the boundary where an inflow boundary condition must be prescribed. The excess of equations over unknowns is

$$N_{\mathrm{Eq}}-N_{\mathrm{Un}}=C-V+V_{\mathrm{b,in}}=\tfrac{1}{3}(E_{\mathrm{i}}-E_{\mathrm{b}})+V_{\mathrm{b,in}}-1$$

which is normally positive, so that all of the residuals cannot be driven to zero. With moving nodes the number of unknowns is about $3V$, so that

$$N_{\mathrm{Eq}}-N_{\mathrm{Un}}\simeq C-3V=-(E_{\mathrm{i}}+5E_{\mathrm{b}})/3-3,$$

which is negative whenever we have more than one cell. There are now many ways to make all of the residuals vanish.

With a 2×2 system and a moving grid, there are $2C$ equations, and about $4V$ unknowns. Again there are many ways to achieve zero residuals.

3. A MESH MOVEMENT SCHEME

Consider minimizing the functional

$$\mathscr{F}=\tfrac{1}{2}\sum_T(\phi^T)'\mathbf{Q}^T\phi^T \tag{4}$$

where the prime denotes a transpose and $\mathbf{Q}^T$ denotes a positive symmetric matrix, not necessarily the same for every element. Straightforward minimization of $\mathscr{F}$ with respect to the arguments of ϕ^T via steepest descent gives a distributive scheme,

$$\delta\mathbf{u}=-\omega_u\mathbf{Q}^T\frac{\partial\phi^T}{\partial\mathbf{u}}\,\phi^T \tag{5}$$

$$\delta\mathbf{x}=-\omega_x\mathbf{Q}^T\frac{\partial\phi^T}{\partial\mathbf{x}}\,\phi^T \tag{6}$$

where $\omega_{u,x}$ are relaxation factors. It is interesting to see how this applies to the simple case of linear advection (1) with $\mathbf{Q}^T=\mathbf{I}$. Each mesh point moves normal to the characteristic direction [9]. Each triangle also attempts to reduce its own area but to leave its centroid

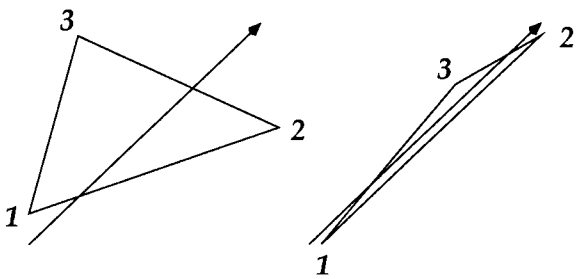

Figure 3. The fluctuation is just the integrated residual over an element. For linear advection it vanishes if one side satisfies the characteristic condition, regardless of the position of or solution at the third vertex.

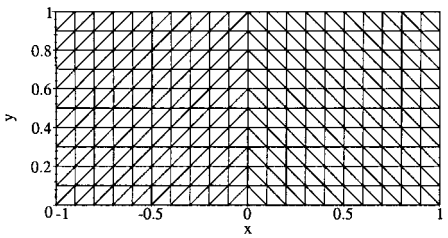

Figure 4. Initial grid for a circular advection problem.

fixed. A particular node is pulled by the wishes of each neighbouring triangle, responding most strongly to those having the largest residuals. Convergence is achieved when each triangle has one side aligned with the characteristic direction. If the boundary nodes are fixed then each node located on the inflow portion of the boundary will be the source of a characteristic line of grid points. The first successful computation is shown in Figures 4 and 5, reproduced from Reference [9] The problem is advection in a circle

$$\partial_t u + y\partial_x u - x\partial_y u = 0$$

with a very sharp hat function input at the lower left boundary. A very striking feature of the results is that only that part of the grid experiencing non-zero residuals at any stage gets to be adapted. In the final grid, those paths that carry information become perfect circles and the exact solution is obtained.

An example of application to a linear 2×2 system is given in Figure 6 where the governing equations are

$$\partial_x u - \partial_y v = 0 \tag{7}$$

$$\partial_x v - \partial_y u = 0 \tag{8}$$

which describe small disturbances to an inviscid stream travelling supersonically at $M = \sqrt{2}$; there are characteristic directions $\mathrm{d}y/\mathrm{d}x = \pm 1$. The boundary conditions are that $v = 0$ on the upper and lower walls, with inflow $u = 1, v = 0.1$ on the left; the problem is that of flow entering a duct at a slight inclination. The initial grid, shown at the left, is a 'good' grid

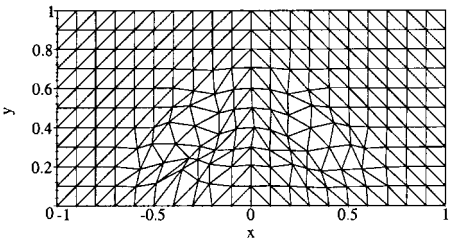

Figure 5. Final grid for a circular advection problem.

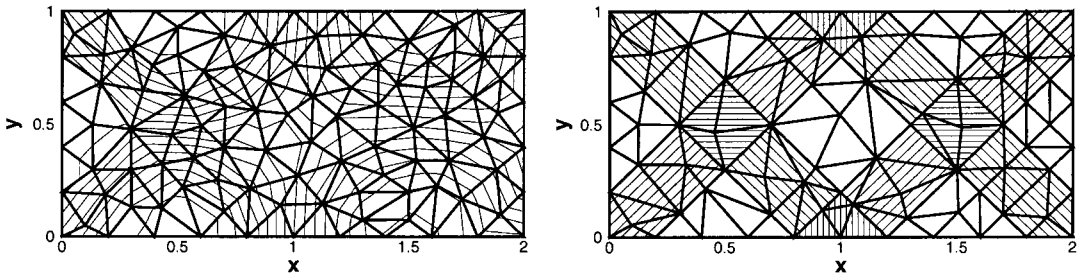

Figure 6. The solution to a simple supersonic flow problem. At left is the initial grid (heavy lines) and the contours of u as computed on that grid. At right is the grid and solution after adaptation.

but not particularly appropriate to the problem. When it is allowed to adapt, all of the grid lines that carry information become aligned with one of the characteristics. The solution is exact, for the given boundary conditions. A minor problem was that we found sometimes that two element edges would compete to represent the same characteristic. This was resolved by deleting grid points whenever the areas of elements became too small.

The actual resolution of the discontinuities can be made arbitrarily precise by allowing the elements to degenerate to zero area; the argument that the residual vanishes when the characteristic equation vanishes along one side does not depend in any way on the value at or location of the third vertex. Prescribing a discontinuity on the boundary allows a discontinuity to propagate into the interior.

4. DEGENERATE ELEMENTS AND ADAPTIVE QUADRATURE

Problems arise in applying the idea of mesh movement to non-linear hyperbolic problems. Elements that try to align their edges with characteristic directions experience difficulty when these directions intersect, as they do at shocks. We were unable to carry the adaptive grids to a converged state, nor apparently were the authors of Reference [11]. But the possibility of success is hinted at by the fact [10] that degenerate elements exist that recognize non-linear shockwaves. The key is the exact form of quadrature employed. To fix ideas, suppose that we have a system of non-linear conservation laws of the form

$$\partial_x \mathbf{F}(\mathbf{w}) + \partial_y \mathbf{G}(\mathbf{w}) = 0 \tag{9}$$

where the fluxes $\mathbf{F}, \mathbf{G}$ are non-linear functions of some state vector $\mathbf{w}$. The residual will be

$$\phi^T = \iint \partial_x \mathbf{F}(\mathbf{w}) + \partial_y \mathbf{G}(\mathbf{w})\,\mathrm{d}x\,\mathrm{d}y$$
$$= \oint (\mathbf{F}(\mathbf{w})\,\mathrm{d}y - \mathbf{G}(\mathbf{w})\,\mathrm{d}x)$$

Exactly how are we to do the contour integral? Along any particular side we have to evaluate the integral

$$\int_a^b (\mathbf{F}(\mathbf{w})\,\mathrm{d}y - \mathbf{G}(\mathbf{w})\,\mathrm{d}x)$$

using information only from the two end-points. Apparently only the Trapezium Rule will work. However, the Trapezium Rule assumes that the integrand varies linearly over the interval $\{a, b\}$, and this cannot be true since $\mathbf{F}, \mathbf{G}$ are each non-linear functions of $\mathbf{w}$. A 'finite-element' approach would be to assume that *some* variable changes linearly, say $\mathbf{w}$ itself, and then integrate each term on that assumption. For example if the non-linearity is quadratic, $\mathbf{F}(\mathbf{w}) = \mathbf{w}'\mathbf{C}\mathbf{w}, \mathbf{G}(\mathbf{w}) = \mathbf{w}'\mathbf{D}\mathbf{w}$, we obtain

$$\int_a^b (\mathbf{F}(\mathbf{w})\,\mathrm{d}y - \mathbf{G}(\mathbf{w})\,\mathrm{d}x) = \frac{y_b - y_a}{3}\,[\mathbf{w}_a'\mathbf{C}\mathbf{w}_a + \mathbf{w}_b'\mathbf{C}\mathbf{w}_b + \mathbf{w}_a'\mathbf{C}\mathbf{w}_b]$$
$$- \frac{x_b - x_a}{3}\,[\mathbf{w}_a'\mathbf{D}\mathbf{w}_a + \mathbf{w}_b'\mathbf{D}\mathbf{w}_b + \mathbf{w}_a'\mathbf{D}\mathbf{w}_b] \tag{10}$$

In fact from the point of view of accuracy alone, there is a single-parameter family of second-order quadratures;

$$\int_a^b (\mathbf{F}(\mathbf{w})\,\mathrm{d}y - \mathbf{G}(\mathbf{w})\,\mathrm{d}x) = (y_b - y_a)\left[\frac{\lambda}{2}\,(\mathbf{w}_a'\mathbf{C}\mathbf{w}_a + \mathbf{w}_b'\mathbf{C}\mathbf{w}_b) + (1-\lambda)\mathbf{w}_a'\mathbf{C}\mathbf{w}_b\right]$$
$$- (x_b - x_a)\left[\frac{\lambda}{2}\,(\mathbf{w}_a'\mathbf{D}\mathbf{w}_a + \mathbf{w}_b'\mathbf{D}\mathbf{w}_b) + (1-\lambda)\mathbf{w}_a'\mathbf{D}\mathbf{w}_b\right] \tag{11}$$

The difference between the answers obtained from any two members of the family is proportional to $(\mathbf{w}_a - \mathbf{w}_b)^2$. The consistent quadrature corresponds to $\lambda = \frac{2}{3}$, but we will now see that the inconsistent quadrature within $\lambda = 1$ has some striking merits.

The residual that follows from taking $\lambda = 1$ can be written in various permutations, one of which is (compare (3))

$$\phi^T = \tfrac{1}{2}[(x_2 - x_3)(\mathbf{G}_2 - \mathbf{G}_1) - (y_2 - y_3)(\mathbf{F}_2 - \mathbf{F}_1)]$$
$$- \tfrac{1}{2}[(x_2 - x_1)(\mathbf{G}_2 - \mathbf{G}_3) - (y_2 - y_1)(\mathbf{F}_2 - \mathbf{F}_3)] \tag{12}$$

Suppose that vertices 1 and 2 lie on the same side of a shock discontinuity. Then the first term vanishes and the second term vanishes if the Rankine–Hugoniot conditions are satisfied

for a jump whose slope coincides with that of the side 12, Moreover, it is not hard to show that only the inconsistent formula with $\lambda = 1$ has this intriguing property.

The possibility of 'shock' elements was noted in Reference [10] but at that time no successful algorithm had been found for moving the nodes to create them. Baines *et al.* [1, 2] subsequently devised a method for manually flagging certain elements in a fixed-grid computation and applied special procedures to them. It would be nice, though, if the procedures for shock and regular elements could be the same. Also, there is no guarantee that the method described will not yield rarefaction shocks.

4.1. A digression concerning entropy

Consider the simpler problem of the one-dimensional Burgers' Equation

$$\partial_t u + \partial_x (u^2/2) = 0$$

solved by a central-differencing scheme

$$u_j^{n+1} = u_j^n - \frac{\Delta t}{\Delta x} [f_{j+1/2}^n - f_{j-1/2}^n]$$

where f is the numerical flux function

$$f_{j+1/2}^n = \frac{1}{2} \lambda_{j+1/2} [(u_j^n)^2 + (u_{j+1}^n)^2] + (1 - \lambda_{j+1/2}) u_j^n u_{j+1}^n$$

In the semi-discrete limit, for data whose variation has compact support, consider the rate of increase of a quadratic entropy

$$\begin{aligned} \frac{\mathrm{d}}{\mathrm{d}t} \sum_j \frac{1}{2} u_j^2 &= \sum_j u_j \frac{\mathrm{d}}{\mathrm{d}t} u_j \\ &= -\frac{1}{2} \sum_j \lambda_{j+1/2} u_j [(u_j^n)^2 + (u_{j+1}^n)^2] + \frac{1}{2} \sum_j \lambda_{j-1/2} u_j [(u_{j-1}^n)^2 + (u_j^n)^2] \\ &\quad - \sum_j (1 - \lambda_{j+1/2}) u_j^2 u_{j+1} + \sum_j (1 - \lambda_{j-1/2}) u_j^2 u_{j-1} \end{aligned}$$

After shifting indices, this can be written as

$$\frac{\mathrm{d}}{\mathrm{d}t} \sum_j \frac{1}{2} u_j^2 = \sum_j \left(\frac{\lambda_{j+1/2}}{2} - \frac{1}{3} \right) (u_{j+1} - u_j)^3 \tag{13}$$

The method *conserves* entropy if $\lambda = 2/3$. However, *reduction* of entropy requires that the parameter λ be *adaptive*. It must be $< 2/3$ if the data is expansive ($u_{j+1} > u_j$), but $> 2/3$ if the data is compressive. We have not yet made a theoretical analogy with the *multi*dimensional problem, but this one-dimensional result is striking and suggestive.

4.2. The adaptive quadrature

Experimenting with very simple two-dimensional fluctuation-splitting on fixed grids to solve the problem,

$$\partial_y u + \partial_x (u^2/2) = 0$$

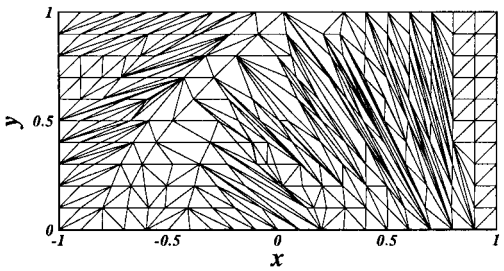

Figure 7. Adapted grid for Burgers' equation problem featuring curved shock.

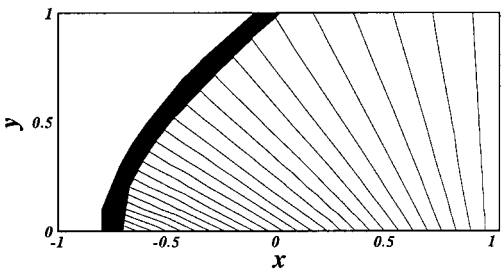

Figure 8. Solution with curvilinear shock on adapted grid.

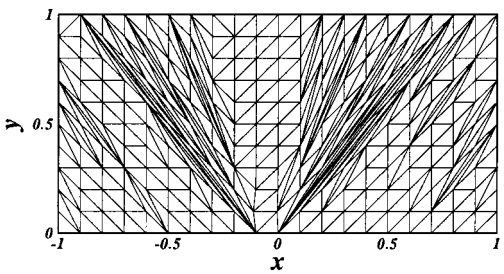

Figure 9. Adapted grid for Burgers' equation problem featuring expansion.

as the steady state of a time-dependent problem, confirmed that the solution depends strongly on the form of quadrature. With λ chosen $>2/3$ any shocks were crisply resolved, but rarefaction shocks were commonplace. With λ chosen $<2/3$ rarefaction shocks disappeared, but shocks were rather diffused. Much the best results were obtained using an adaptive quadrature. We took simply $\lambda=1$ for compressive elements, and $\lambda=0$ for expansive elements. Simultaneously, this strategy took care of most of the problems with the mesh movement.

The distinction between compressive and expansive elements was made by considering, for each element, the quantity $\operatorname{div}\Lambda$, where Λ is the vector field corresponding to the characteristic velocities in this case $\Lambda=(u,1)$.

Figures 7–10 show the outcome of two adaptive grid calculations, one of them featuring a curved shock and the other a rarefaction fan. In both cases a very large number of

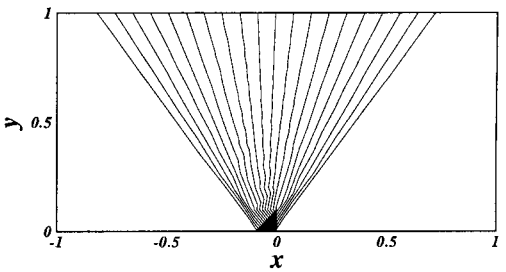

Figure 10. Solution with expansion on adapted grid.

element edges align themselves with the local characteristic direction and the solution quality is excellent. In particular, the shockwave maintains itself as a jump over only one element, with a width that remains fixed by the width over which the discontinuity was given in the data.

The chief problem remaining in these calculations is an excessive number of points in the *smooth* part of the flow. The difficulty is that a well-adapted grid could operate with many fewer points than were supplied initially. We did implement a node removal strategy, based on removing elements having less than some threshold area, but there are still too many. We hope to develop an economical measure of *grid point utility* and use this to remove nodes. Another helpful feature would be to allow points on the outflow boundary to move along the boundary, because the ideal grid would have one outflow node so placed to receive the information from every inflow node.

5. ELLIPTIC PROBLEMS

We have particularly studied the Cauchy–Riemann system

$$\begin{aligned} \partial_x u + \partial_y v &= 0 \\ \partial_x v - \partial_y u &= 0 \end{aligned} \tag{14}$$

One would like to drive the cell residuals to zero, but this is only possible in special cases. For a 2×2 system without grid movement the problem is strongly overdetermined. With grid movement, the counting is delicate, depending on the strategy at the boundaries, but is usually just overdetermined. A tempting proposal is to minimize the residuals in some norm. It is pointed out in Reference [9] that the choice of norm

$$\mathscr{F} = \sum_T \frac{(\Delta^T)^2 + (\Omega^T)^2}{S^T} \tag{15}$$

where Δ^T, Ω^T are the element residuals for divergence and curl, respectively, and S^T is the area of the triangle, reproduces, in the interior of the domain, the standard Galerkin method for the Laplace equations $\nabla^2 u = \nabla^2 v = 0$. Moreover, a theorem in Reference [7] guarantees that residual-minimization is a scheme that converges under mesh refinement.

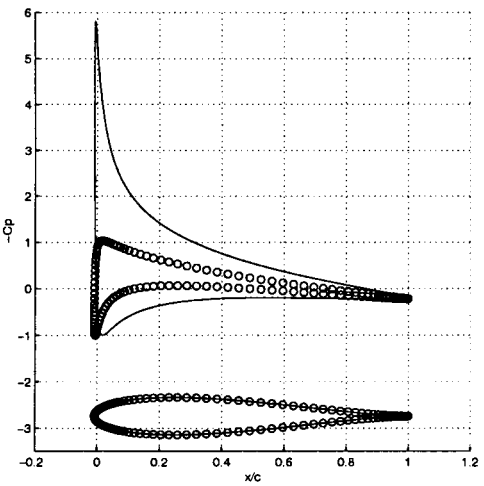

Figure 11. Airfoil solution obtained from 'second-order' least-squares solution to Cauchy–Riemann equations on a grid with 160×80 nodes.

Our experience with this method was extremely disappointing. We looked at the exterior incompressible flow round airfoils, for which exact solutions are available via conformal mapping. We obtained good solutions to the non-lifting flow round symmetric airfoils at zero angle of attack, but Figure 11 is depressingly typical of our results for lifting cases. The pressure difference between the upper and lower surface is badly underpredicted, as is therefore the lift. Since the residuals are being evaluated by piecewise linear elements one might expect second-order accuracy for this calculation, but a convergence study revealed that not even first order was achieved. The results remained poor even though we prescribed the exact solution on the outer boundary, so that the circulation was correct there. The low prediction of lift implies, however, that the circulation is not correct for contours close to the airfoil. This means that the average value of vorticity between the airfoil and the outer boundary is not zero, and this seems to correspond to a weakness of residual-minimization methods. Merely ensuring that the residuals are small does not imply that their mean is zero, so there is no demonstration of global accuracy for the circulation. It should be noted that the proof of convergence in Reference [7] does not lead to an error estimate. Significantly better results were obtained by removing the weight S^T in the above norm, although no convincing explanation for this presents itself.

We explain our observations by remarking that there is no strong reason why the residuals should measure the error. Indeed, for linear elements, the error must involve second derivatives, concerning which the residuals have nothing to say. Practically, the point is made by the fact that allowing nodal movement significantly reduced the residuals, but had only minor effects on the error; they produced instead a grid on which the same bad solution merely looked better. A more conventional method worked better. A Lax–Wendroff method can be put into the form of a residual distribution scheme. At convergence it forces the sum of the residuals at each node to vanish, modulo a small dissipative term. On the same grid it gave the very acceptable results in Figure 12.

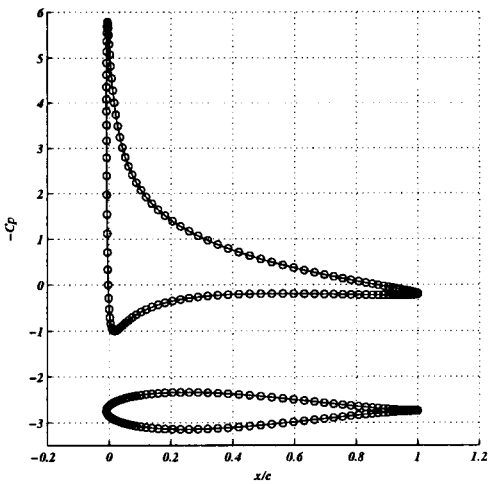

Figure 12. Airfoil solution obtained from Lax–Wendroff solution to Cauchy–Riemann equations on a grid with 160×80 nodes.

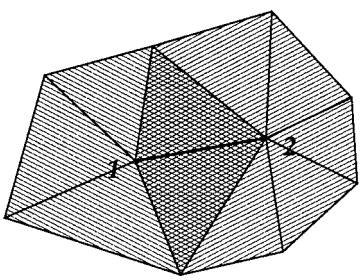

Figure 13. To evaluate the flux over the edge 12, a curvature correction is made using the derivatives at each end. The two derivatives are found using the shaded control volumes.

5.1. Third-order accuracy

A major enhancement to the Fluctuation-Splitting Method has recently been made by Caraeni *et al.* [4]. The error in integrating along one side of an element using the Trapezium Rule is $h^3/24$ times the second derivative of the integrand in the direction of that edge. By estimating and subtracting that error the residual can be made third-order accurate. We follow Caraeni *et al.* by finding the second derivative along the edge as the difference between two first derivatives evaluated at the vertices. These derivatives are obtained by applying Gauss' Theorem to the control volumes formed by the elements surrounding each endpoint of the edge (see Figure 13). In Reference [4] the update is performed, on a fixed mesh, using a Lax Wendroff method, but we have found that with this version of the residual (as modified by the curvature terms) equally good solutions are obtained by minimization. Without yet having made a complete analysis, it seems that these third-order residuals do contain information about the error, so that moving the nodes to reduce them could make sense. Indeed we have found this to be the case.

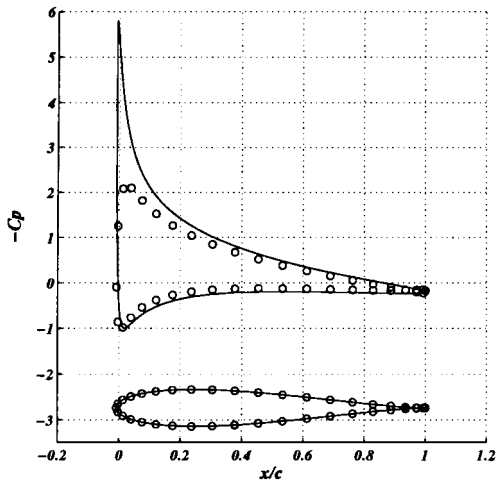

Figure 14. Airfoil solution obtained from third-order least squares solution to Cauchy–Riemann equations on a fixed grid with 40×20 nodes.

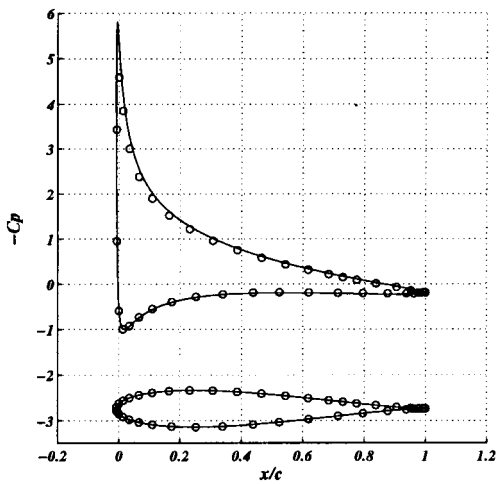

Figure 15. Airfoil solution obtained from third-order least-squares solution to Cauchy–Riemann equations on a adapted grid with 40×20 nodes.

Figure 14 shows the solution on a rather coarse 40×20 grid obtained with the third-order least-squares scheme. It is reasonable considering the lack of resolution, but when the node placement is optimized to minimize the residuals, the solution is dramatically better, as shown in Figure 15.

The initial grid for this calculation was the rather nice-looking one shown in Figure 16. The optimization procedure yielded the slightly less regular grid shown in Figure 17, which has the grid density increased close to the airfoil, and especially in the critical leading- and trailing-edge regions.

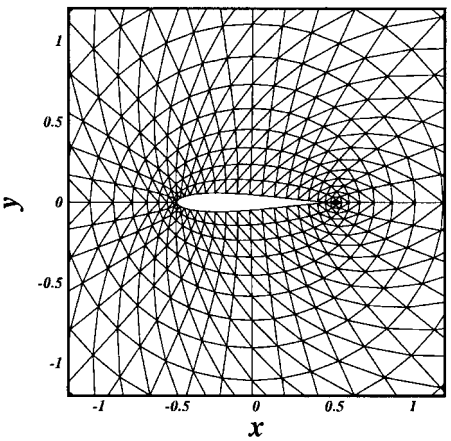

Figure 16. Initial grid for the airfoil problem with 40×20 nodes.

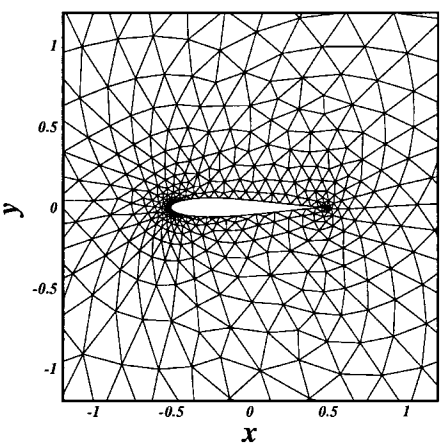

Figure 17. Adapted grid for the airfoil problem with 40×20 nodes.

6. CONCLUSIONS AND FUTURE WORK

When solving steady-state problems in two dimensions, optimizing the grids so as to minimize element residuals can vastly reduce the storage requirements, but the correct norm in which to minimize can involve rather subtle issues, even in the simple cases considered here. In the non-linear hyperbolic case, the quadrature must be such that shocks can be recognized, but use of a single quadrature formula appears to give an unstable method. In the linear elliptic case, residuals based on linear elements do not seem to contain enough information about the errors, but residuals containing curvature corrections are extremely successful.

The payoff from this research is most likely to be felt in three-dimensional calculations. However, work on the distinctively three-dimensional aspects has barely begun. The second author has coded a non-uniform advection problem analogous to Figure 5 in three dimensions,

and again an exact solution is obtained when the grid becomes characteristic. Degenerate shock elements can be found in three dimensions, but no computations have been made with them.

So far, the entire emphasis of the research has been to question whether the grid resources currently consumed by CFD codes are really needed. We ourselves have given little attention to the issue of generating more efficient grids in an efficient way. The least-square procedures we employ are certainly not efficient; the grid in Figure 5 takes many thousands of iterations to achieve. However, essentially the same grid was generated by Baines *et al.* [1] in a few tens of iterations by using upwinded relaxation.

To achieve any practical impact, equation sets with mixed behaviour, such as the subsonic Euler equations with elliptic and hyperbolic simultaneously present, need to be considered. A reason for feeling optimistic about this is that the grid only responds to non-zero residuals. The residuals can be decomposed into their elliptic and hyperbolic components [8], and will respond more strongly to whichever is locally dominant. We hope to begin practical tests of such a method in the near future.

REFERENCES

1. Baines MJ, Leary SJ, Hubbard ME. A finite-volume method for steady hyperbolic equations. In *Finite Volumes for Complex Applications II*, Vilsmeier, Benkhaldoun, Hanel, Duisberg (eds). Hermes, 1999.
2. Baines MJ, Leary SJ, Hubbard ME. Multidimensional least squares fluctuation distribution schemes with adaptive mesh movement for steady hyperbolic equations. *SIAM Journal on Scientific Computing*, submitted for publication.
3. Castro-Diaz MJ, Hecht F, Mohammedi B, Pironneau O. Anisotropic unstructured mesh adaptation for flow simulations. *International Journal for Numerical Methods in Fluids* 1997; **20**:191.
4. Caraeni D, Caraeni M, Fuchs L. A parallel multidimensional upwind algorithm for LES. *AIAA Paper* 2001-2547, 15th AIAA CFD Meeting, Anaheim, 2001.
5. Deconinck H, Roe PL, Struijs R. A multidimensional generalisation of Roe's flux difference splitter for the Euler equations. *Computers and Fluids* 1993; **22**:215.
6. Habashi WG. *et al.* Anisotropic mesh adaptation: toward user-independent, mesh-independent and solver-independent CFD. Part I: general principles. *International Journal for Numerical Methods in Fluids* 2000; **32**:725.
7. Jiang B. *The Least-Squares Finite-Element Method-Theory and Applications in Computational Fluid Dynamics and Electromagnetics*. Springer: Berlin, 1998.
8. Rad M, Roe PL. An Euler code that can preserve potential flow. In *Finite Volumes for Complex Applications*, Vilsmeier, Benkhaldoun, Hanel, Duisberg (eds). Hermes, 1999.
9. Roe PL. Compounded of many simples, reflections on the role of model problems. In *CFD, workshop on barriers and challenges in Computational Fluid Dynamics*, NASA, Langley, August, 1996, Venkatakrishnan, Salas, Chakravarthy (eds). Kluwer, Academic Publishers: Dordrecht, 1998.
10. Roe PL. Fluctuation splitting on optimal grids. AIAA CFD Meeting, Snowmass, CO, June 1997.
11. Wood WA, Kleb WL. On multidimensional unstructured mesh adaptation. *AIAA 14th CFD Conference*, June 1999, Paper 99-3254.

